Drug Discovery in Flow | Hot Paper

DOI: 10.1002/anie.201309301

Seamless Integration of Dose-Response Screening and Flow Chemistry: Efficient Generation of Structure–Activity Relationship Data of β-Secretase (BACE1) Inhibitors**

Michael Werner, Christoph Kuratli, Rainer E. Martin,* Remo Hochstrasser, David Wechsler, Thilo Enderle, Alexander I. Alanine, and Horst Vogel*

Abstract: *Drug discovery is a multifaceted endeavor encompassing as its core element the generation of structure-activity relationship (SAR) data by repeated chemical synthesis and biological testing of tailored molecules. Herein, we report on the development of a flow-based biochemical assay and its seamless integration into a fully automated system comprising flow chemical synthesis, purification and in-line quantification of compound concentration. This novel synthesis-screening platform enables to obtain SAR data on b-secretase (BACE1) inhibitors at an unprecedented cycle time of only 1 h instead of several days. Full integration and automation of industrial processes have always led to productivity gains and cost reductions, and this work demonstrates how applying these concepts to SAR generation may lead to a more efficient drug discovery process.*

The identification of a lead compound through iterative generation of structure–activity relationship (SAR) data is at the core of early-stage drug discovery.[1] A complete SAR cycle is composed of organic synthesis, compound purification, chemical structure confirmation, biological evaluation, and data analysis. The workflow for generation of SAR data is usually distributed across highly specialized facilities and must account for time-consuming compound management and transfer steps. As a result, biological data on a new chemical structure is rarely available prior to one week after its synthesis. Parallelization of chemical synthesis and bioassaying has been the most common solution but remains largely cost-intensive owing to lack of real-time feedback and consequential generation of irrelevant chemical examples.[2] Thus, there is an imminent unmet need for merging chemical, analytical, and biological procedures into a single continuous process that minimizes spatio-temporal barriers and fosters a cost-efficient lead discovery process.[3] Herein, we demonstrate the seamless integration of a purposely developed flow-compatible biological assay into a fully automated platform consisting of flow chemical synthesis and in-line compound purification and quantification. We demonstrate the execution of complete SAR cycles within 60 min from injection of the starting materials to generation of the half-maximal inhibitory concentration (IC_{50}) against a given biological target. Finally, we report the successful validation of our approach by generating SAR data for two different aniline building blocks coupled to a selection of carboxylic acids targeting the inhibition of β-secretase, which is currently a key and challenging target in Alzheimer's research, where progress is largely driven by synthesis.[4]

Despite recent progress in automation and integration of chemical and biological methods,[5–16] the lack of a direct in-line method for compound profiling in dose-response format has prevented the emergence of truly seamless processes.[2,17,18] Therefore, we first developed a continuous-flow procedure that generates a compound concentration gradient of six orders of magnitude from a single injection followed by incorporation of assay reagents. Formation of the gradient was achieved in a thin capillary controlled by Taylor dispersion,[19] a fluid mechanical effect previously exploited for flow-injection-based chemical analyses.[20] Addition of the assay reagents (herein BACE1 enzyme and substrate) to the compound gradient was performed on a specially designed glass chip (Figure 1 A) by merging the compound gradient stream with the enzyme and substrate streams at a distinct ratio, which was subsequently homogenized through a split-and-recombine mixer. All of the flows were stopped when the rising edge of the compound gradient filled the holding line for incubation of the assay reaction. The current BACE1 inhibition assay is based on fluorescence dequenching (Supporting Information, Figure S2) and is constrained to small assay window and low catalytic activity.[21] We therefore set up a robust kinetic readout by recording the slope of fluorescence increase at more than 100 distinct positions, that is, compound concentrations, along the holding line and at four different time points. For determination of IC_{50} values, the compound concentration had to be calibrated for each of the scan positions. In our system, the final compound concentrations depend primarily on convective forces, that is, on the

[*] Dr. M. Werner, C. Kuratli, Dr. R. E. Martin, Dr. R. Hochstrasser, D. Wechsler, Dr. T. Enderle, Dr. A. I. Alanine
Medicinal Chemistry, Small Molecule Research, Pharma Research & Early Development (pRED), F. Hoffmann-La Roche AG
Grenzacherstrasse 124, 4070 Basel (Switzerland)
E-mail: michael.werner@roche.com
rainer_e.martin@roche.com

Prof. Dr. H. Vogel
Institute of Chemical Sciences and Engineering
Swiss Federal Institute of Technology of Lausanne (EPFL)
Station 6, 1015 Lausanne (Switzerland)

[**] We are grateful to Dr. Hans Hilpert for helpful discussions, Roland Humm for providing building blocks **A** and **B**, Daniel Zimmerli, Roger Werder, and Tom Kissling for technical support, as well as Dr. Annie Moisan and Prof. Klaus Müller for critical reading of the manuscript.

Supporting information for this article is available on the WWW under http://dx.doi.org/10.1002/anie.201309301.

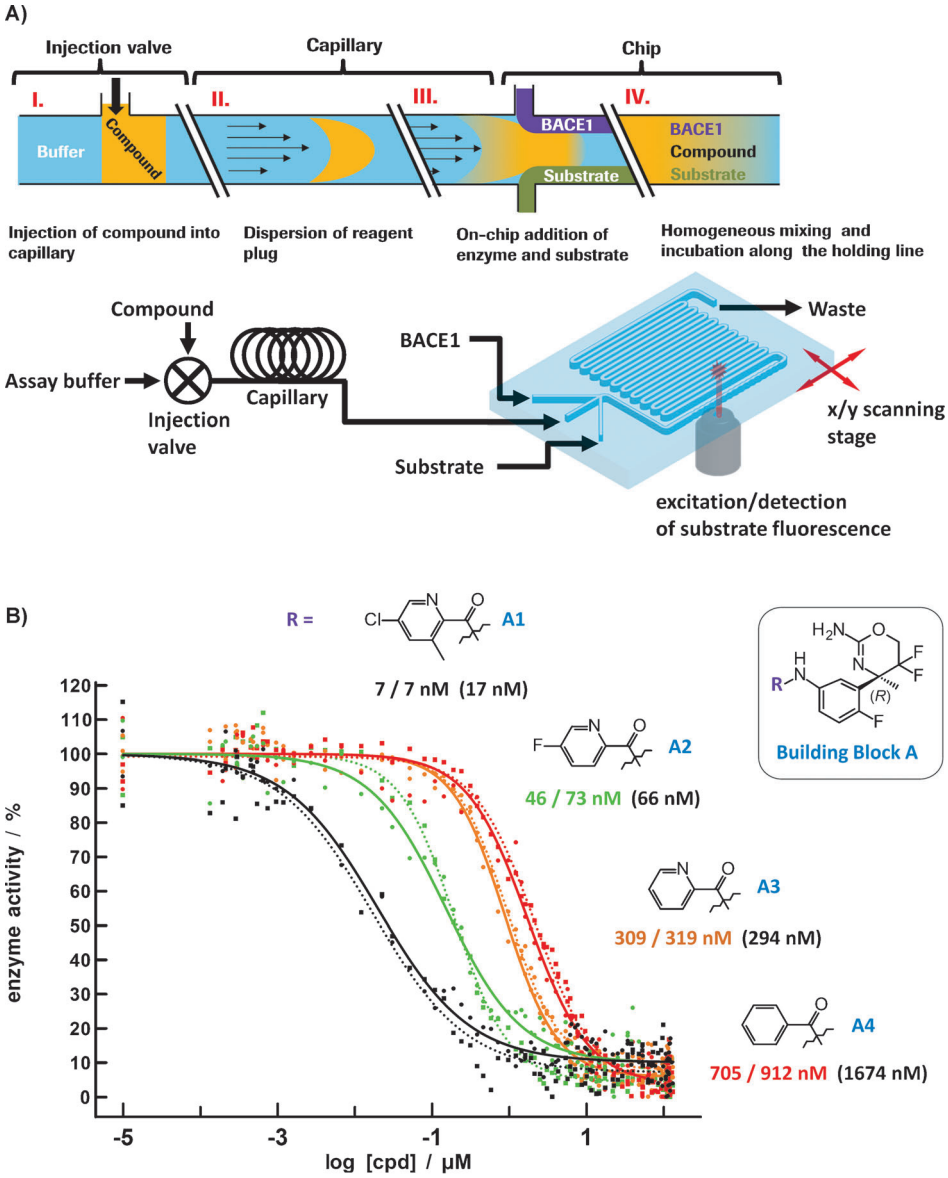

Figure 1. A) Illustration of the flow-based assay procedure and outline of the employed microfluidic setup. B) Dose-response curves and associated potencies obtained for screening **A1**–**A4** in duplicate against BACE1. In parentheses: corresponding wellplate-based average potency values.

prevalent flow profile while compound structure-dependent diffusive forces can be neglected (Supporting Information, Section S2.5). Consequently, the concentration gradient was calibrated with a single reference compound (fluorescein, 10 mM), the concentration of which was indirectly measured by laser-induced fluorescence. As fluorescein displayed a weak fluorescence under acidic assay conditions, all of the buffer solutions were replaced by an alkaline borate buffer, whereas other parameters remained unchanged (Supporting Information, Section S2.6). Fluorescence intensities were converted into concentration values by means of a calibration using known fluorescein concentrations. An average calibration gradient was generated from three independent runs by calculating the arithmetic mean value for each scan position. The dynamic range was defined by the detection (ca. 100 pM) and saturation limits (ca. 100 µM), respectively (Supporting Information, Figure S3). This chip-based enzyme inhibition assay was validated using a set of four different BACE1 inhibitors (Figure 1B), which were assayed in duplicate. For evaluation of the accuracy of the measured chip-based potency values, the usual scattering of replicates around their average values (up to a factor of three) observed for this assay type in 384-wellplates (15-fold serial dilution) was taken into account. Accordingly, the obtained average potencies reflected well the potency values generated by classical screening, while approximately four times less material per data-point was consumed. Notably, compared to state-of-the art flow assays, which are limited by the addressable dose range or the incompatibility with hydrophobic assay constituents, the reported assay covers an unprecedented dose range of six orders of magnitude and is in principle amenable to all fluorescence screening assays.[22–25]

The bioassay setup was subsequently coupled to a flow-chemistry platform allowing in-line purification by preparative HPLC, compound identification by LC-MS, and quantification using a calibrated evaporative light-scattering detector (ELSD). Initially, product fractions from the LC-MS unit were collected in an open reservoir (Supporting Information, Section S3.1.1). This semi-integrated yet fully automated configuration enabled evaluating the accuracy of the ELSD calibration by off-line quantification of each product fraction using standard gravimetric (GA) and ^{1}H NMR spectroscopic analysis. For validation of the platform, a diverse set of 20 different BACE1 inhibitors was synthesized from two different aniline building blocks (**A** and **B**) by coupling each template to 10 different carboxylic acids (Figure 2A). These side-chains **1**–**10** were selected based on recently published BACE1 inhibition values to span the entire potency range from highly active ($IC_{50} < 100$ nM) to modestly active ($IC_{50} \approx 0.1$–1 µM) and weakly active compounds ($IC_{50} > 1$ µM).[4,26] The amidation reactions were conducted on a Vapourtec R4 flow synthesizer coupled to a Gilson liquid handler for automated sample handling. The use of 4-(4,6-dimethoxy-

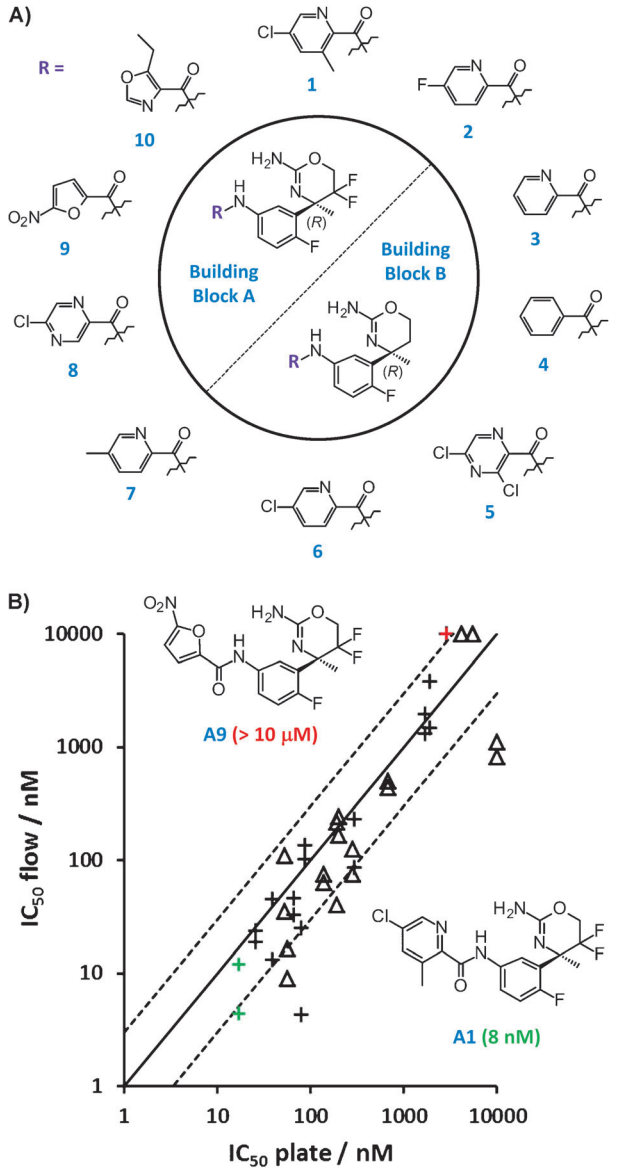

Figure 2. A) Chemical structures of the two libraries of BACE1 inhibitors (each comprising 10 compounds) used for validation of the semi-integrated and the fully integrated platform. B) Inhibition potencies obtained upon screening of the full library against BACE1 using the semi-integrated platform. IC_{50} values are compared to the respective values obtained by classical synthesis in batch and wellplate-based screening (+ **A1**–**A10**; △ **B1**–**B10**). Chemical structures for the most potent inhibitor (green markers) as well as for one of the inactive compounds (red markers) are highlighted. Dotted lines: ±300% intervals indicating the typical scattering of replicates around their average values in classical wellplate-based screening.

1,3,5-triazin-2-yl)-4-morpholinium tetrafluoroborate (DMTMMT) as the coupling reagent enabled amide formation preferentially at the aniline nitrogen atom and only to a minor extent at the undesired, but (owing to its higher basicity) intrinsically more reactive amino oxazine moiety.[4] The purified compounds **A1**–**A10** and **B1**–**B10** were isolated by a liquid handler collecting 4–5 mL of product with concentrations ranging from 0.2 mM to 2.1 mM as determined by ^{1}H NMR analysis. Aliquots were subsequently taken by the same liquid handler for purity analysis by LC-MS, quantification by ELSD, and for IC_{50} determination against BACE1. Additional aliquots were manually taken for analysis by GA and ^{1}H NMR spectroscopy, revealing an average error of approximately ±30% and ±40% in the ELSD quantification (Supporting Information, Table S1), respectively. As ELSD calibration was performed using structurally diverse reference compounds and thus applicable to a wide chemical space, these error margins were largely acceptable. The measured IC_{50} values were in good agreement with the values derived by classical methods (batch synthesis, wellplate-based screening) reflected by 70% of the potencies differing less than factor three from the average classically derived values (Figure 2B). Also, 95% of the replicates displayed IC_{50} values differing less than factor three from their average values, demonstrating that the reproducibility of the semi-integrated platform is comparable to classical methods. Interestingly, most potencies derived from the semi-integrated platform were slightly overestimated compared to the classically derived potencies, which is much less of concern as underestimation of IC_{50} values would result in premature exclusion of interesting lead candidates. Similar semi-integrated synthesis and screening platforms have been recently proposed: Guetzoyan et al. have coupled continuous-flow chemical synthesis with a column-based affinity assay,[17] while Desai et al. and Czechtizky et al. have combined commercial flow chemistry setups with classical wellplate-based biochemical assays.[2,18] In these studies chemical synthesis and biological evaluation was coordinated either manually or by using complex and expensive liquid handling robotics. However, a seamless and strictly flow-based interface offers considerable advantages in a drug discovery environment beyond simpler, remote-controllable equipment such as instant transfer of compounds, reduction of costly sample consumption, minimization of contamination sources and safe handling of hazardous compounds. Therefore, we ultimately set out to fully integrate the flow-based bioassay to allow a seamless synthesis-purification-screening process (Figure 3A; Supporting Information, Section S3.1.2). Here, a given product fraction was collected "on the fly" in a separate capillary and moved to a position where the maximum of the Gaussian-type dispersion profile of the fraction was stretched out over the injection loops for the analytical LC-MS/ELSD unit and the bioassay, respectively. Consequently, samples for both quantification and IC_{50} generation were of nearly identical composition. For validation of the fully integrated platform, SAR data was generated for a subset of the libraries shown in Figure 2A. Owing to sample-taking from the region of highest product concentration, it was possible to reduce the amount of aniline building blocks to 2.5 mg. Remarkably, 71% of the generated IC_{50} values differed less than factor three from the classically derived potencies; similarly, 93% of the IC_{50} values of the replicates were scattered less than factor three around their average values (Figure 3B). Thus, the fully integrated platform yielded reproducible SAR data in good agreement with classical methods. Most importantly, we correctly identified compound **A1** as the most potent BACE1 inhibitor of the library with an average IC_{50} of 12 nM. Synthesis and purification of a compound was accom-

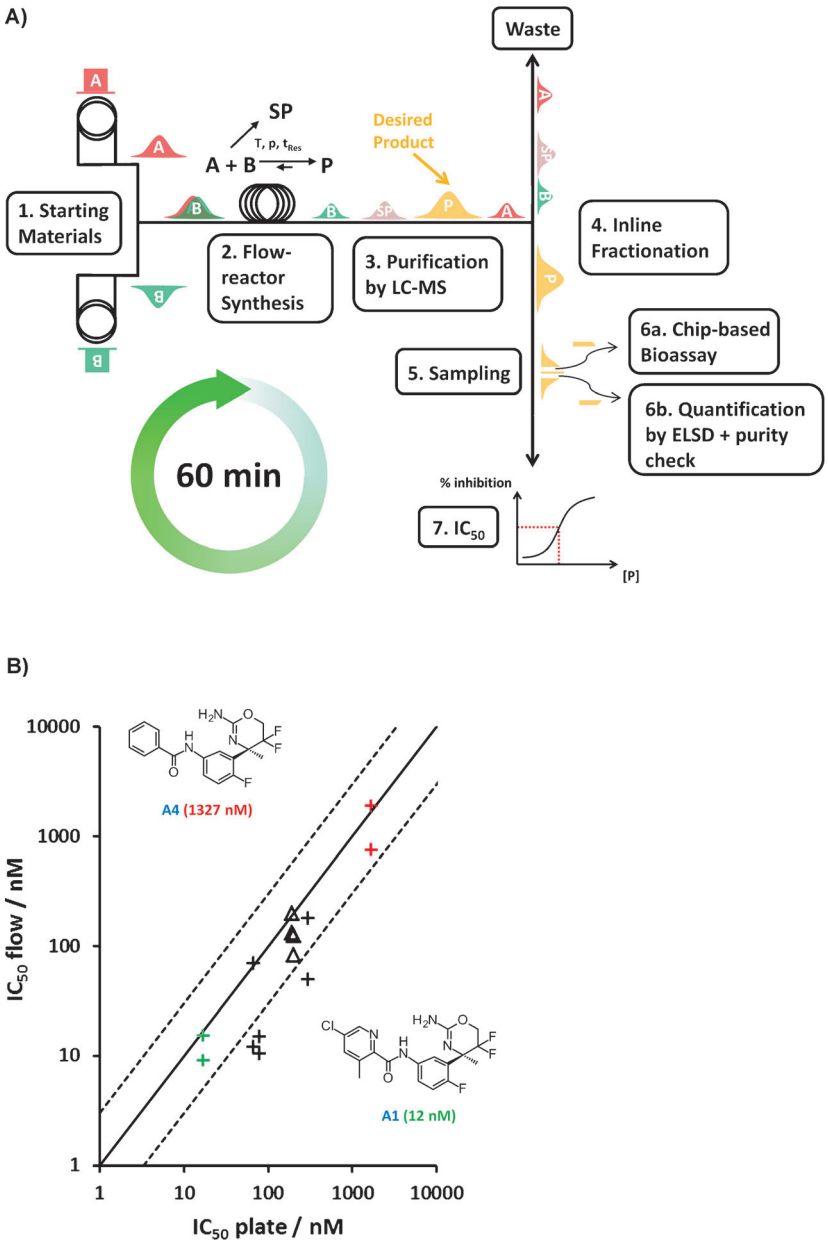

Figure 3. A) The workflow of the fully integrated synthesis and screening platform. Compounds were prepared, purified, quantified, and assayed against BACE1 in a single continuous-flow process (cycle time: 60 min). B) Inhibition potencies obtained upon screening of a subset of the library shown in Figure 2A against BACE1 using the fully integrated platform. IC_{50} values are compared to the respective values obtained by classical synthesis in batch and wellplate-based screening (+ **A1**–**A5**; △ **B2** and **B7**). Chemical structures for the most potent (green markers) as well as for the weakest inhibitor (red markers) are highlighted. Dotted lines: 300% intervals according to Figure 2B.

plished in about 30 min, thus proceeding at the same timescale as the bioassay. As the reusable glass chip was washed after each experiment for about 30 min, the total synthesis-purification-bioassay time for our system was on the order of 60 min. To the best of our knowledge, this is the first time that SAR data for identification and optimization of lead compounds was generated at such high cycle rates.

In summary, drug discovery is a multifaceted endeavor that encompasses as its core elements the repeated chemical synthesis and biological testing of tailored molecules, and here we show for the first time how both worlds can be seamlessly merged. Industrial processes have always benefited from full integration and automation of the individual components they are composed of, in particular through the resulting efficiency gains and cost reductions. This work demonstrates how applying these concepts to the SAR generation workflow may lead to an accelerated and more efficient drug discovery process owing to reduced synthesis-testing cycle times and thus contribute to the pharmaceutical industry's continuous pursuit of enhancing its productivity.[27–29]

Experimental Section

Chip-based enzyme inhibition assay: The experiment was started by loading the loop (internal volume = 70 μL) of a software-controlled injection valve with the compound to be assayed. For validation of the chip-based assay this step was executed manually. For the semi- and fully integrated synthesis-screening experiments, compounds were injected by a liquid handler or transferred directly from the preparative HPLC unit, respectively. The chip was subsequently primed with streams of enzyme (90 nM), substrate (0.9 μM), and assay buffer, each running at a flow rate of 0.8 mL min^{-1}. After 2 min the compound was injected into the dispersion capillary (internal radius = 375 μm, length = 40 cm) without interruption of the flows and dispersed by assay buffer along the capillary. The compound gradient stream entered the chip through the central channel and was merged with streams of enzyme and substrate at equal ratios. A split-and-recombine mixer incorporated close to the inlet channels led to homogeneous mixing of compound, enzyme, and substrate. All of the flows were stopped 46 seconds after compound injection. The mixture was then incubated for 30 min during which substrate fluorescence increase was monitored at 107 positions along the holding line during 4 cycles. For spatial distribution of the scan positions, the variation in the gradient steepness was taken into account, that is, spacing between two scan positions was large where the gradient was flat and small where the gradient was steep. This scanning mode enabled a more regular spreading of data points over the whole dose range. After each experimental run, the chip was washed with distilled water for about 30 min. To establish dose-response curves, the slope of the fluorescence intensity increase over time was calculated for each of the 107 positions and converted into corresponding % values of enzyme activity under the assumption that the maximal fluorescence increase resulted from full enzyme activity while the lowest fluorescence increase resulted from a fully inhibited enzyme. Using the gradient calibration (Supporting Information, Section S2.6) enzyme activities were plotted versus the corresponding fluorescein concentrations and the resulting dose-response curve fitted by a four-parameter Hill equation. Obtained potencies IC_{50}^{0}

were corrected for the mismatch between the initial concentrations of the assayed compounds C_i^C and the initial concentration of the reference compound fluorescein C_i^F according to:

$$IC_{50} = IC_{50}{}^0(C_i^C/C_i^F) \quad (1)$$

Received: October 24, 2013

Keywords: biochemical assays · flow synthesis · lead discovery · medicinal chemistry · microfluidics

[1] K. Bleicher, H. J. Böhm, K. Müller, A. I. Alanine, *Nat. Rev. Drug Discovery* **2003**, *2*, 369 – 378.
[2] B. Desai, K. Dixon, E. Farrant, Q. Feng, K. R. Gibson, W. P. van Hoorn, J. Mills, T. Morgan, D. M. Parry, M. K. Ramjee, C. N. Selway, G. J. Tarver, G. Whitlock, A. G. Wright, *J. Med. Chem.* **2013**, *56*, 3033 – 3047.
[3] S. Y. F. W. Hawkes, M. J. V. Chapela, M. Montembault, *QSAR Comb. Sci.* **2005**, *24*, 712 – 721.
[4] H. Hilpert, W. Guba, T. J. Woltering, W. Wostl, E. Pinard, H. Mauser, A. V. Mayweg, M. Rogers-Evans, R. Humm, D. Krummenacher, T. Muser, C. Schnider, H. Jacobsen, L. Ozmen, A. Bergadano, D. W. Banner, R. Hochstrasser, A. Kuglstatter, P. David-Pierson, H. Fischer, A. Polara, R. Narquizian, *J. Med. Chem.* **2013**, *56*, 3980 – 3995.
[5] C. Wiles, P. Watts, *Future Med. Chem.* **2009**, *1*, 1593 – 1612.
[6] M. Baumann, I. R. Baxendale, S. V. Ley, *Mol. Diversity* **2011**, *15*, 613 – 630.
[7] P. Watts, *Micro Reaction Technology in Organic Synthesis*, CRC, Boca Raton, **2011**.
[8] L. Malet-Sanz, F. Susanne, *J. Med. Chem.* **2012**, *55*, 4062 – 4098.
[9] I. R. Baxendale, *J. Chem. Technol. Biotechnol.* **2013**, *88*, 519 – 552.
[10] V. Hessel, D. Kralisch, N. Kockmann, T. Noel, Q. Wang, *ChemSusChem* **2013**, *6*, 746 – 789.
[11] S. G. Newman, K. F. Jensen, *Green Chem.* **2013**, *15*, 1456 – 1472.
[12] J. Hong, J. B. Edel, A. J. deMello, *Drug Discovery Today* **2009**, *14*, 134 – 146.
[13] L. Y. Yeo, H. C. Chang, P. P. Chan, J. R. Friend, *Small* **2011**, *7*, 12 – 48.
[14] M. L. Kovarik, P. C. Gach, D. M. Ornoff, Y. Wang, J. Balowski, L. Farrag, N. L. Allbritton, *Anal. Chem.* **2012**, *84*, 516 – 540.
[15] P. Neuzi, S. Giselbrecht, K. Lange, T. J. Huang, A. Manz, *Nat. Rev. Drug Discovery* **2012**, *11*, 620 – 632.
[16] M. L. Kovarik, D. M. Ornoff, A. T. Melvin, N. C. Dobes, Y. Wang, A. J. Dickinson, P. C. Gach, P. K. Shah, N. L. Allbritton, *Anal. Chem.* **2013**, *85*, 451 – 472.
[17] L. Guetzoyan, N. Nikbin, I. R. Baxendale, S. V. Ley, *Chem. Sci.* **2013**, *4*, 764 – 769.
[18] W. Czechtizky, J. Dedio, B. Desai, K. Dixon, E. Farrant, Q. X. Feng, T. Morgan, D. M. Parry, M. K. Ramjee, C. N. Selway, T. Schmidt, G. J. Tarver, A. G. Wright, *ACS Med. Chem. Lett.* **2013**, *4*, 768 – 772.
[19] G. Taylor, *Proc. R. Soc. London Ser. A* **1953**, *219*, 186 – 203.
[20] J. Ruzicka, *Anal. Chem.* **1983**, *55*, 1040 – 1053.
[21] F. Gruninger-Leitch, D. Schlatter, E. Kung, P. Nelbock, H. Dobeli, *J. Biol. Chem.* **2002**, *277*, 4687 – 4693.
[22] J. Pihl, J. Sinclair, E. Sahlin, M. Karlsson, F. Petterson, J. Oloffson, O. Orwar, *Anal. Chem.* **2005**, *77*, 3897 – 3903.
[23] L. F. Cai, Y. Zhu, G. S. Du, Q. Fang, *Anal. Chem.* **2012**, *84*, 446 – 452.
[24] O. J. Miller, A. E. Harrak, T. Mangeat, J. C. Baret, L. Frenz, B. E. Debs, E. Mayot, M. L. Samuels, E. K. Rooney, P. Dieu, M. Galvan, D. R. Link, A. D. Griffiths, *Proc. Natl. Acad. Sci. USA* **2012**, *109*, 378 – 383.
[25] Y. Chen, A. Wijaya Gani, S. K. Tang, *Lab Chip* **2012**, *12*, 5093 – 5103.
[26] D. Banner, W. Guba, H. Hilpert, H. Mauser, A. V. Mayweg, R. Narquizian, E. Pinard, E. Power, M. Rogers-Evans, T. J. Woltering, W. Wostl, WO 2011/069934A1, **2011**.
[27] F. Pammolli, L. Magazzini, M. Riccaboni, *Nat. Rev. Drug Discovery* **2011**, *10*, 428 – 438.
[28] M. E. Bunnage, *Nat. Chem. Biol.* **2011**, *7*, 335 – 339.
[29] S. M. Paul, D. S. Mytelka, C. T. Dunwiddie, C. C. Persinger, B. H. Munos, S. R. Lindborg, A. L. Schacht, *Nat. Rev. Drug Discovery* **2010**, *9*, 203 – 214.

